



Ground Motions, Site Amplification and Building Damage at Near Source of the 2006 Yogyakarta, Indonesia Earthquake

Widodo Pawirodikromo 

Received: 12 May 2020 / Accepted: 14 July 2022 / Published online: 21 August 2022
© The Author(s), under exclusive licence to Springer Nature Switzerland AG 2022

Abstract The objective of this study is to ascertain the causes of damage to buildings that occurred due to an earthquake near its source, particularly in the Pleret sub-district in Yogyakarta Special Province Indonesia. This study was conducted because a large percentage of human fatalities and structural collapse occurred during the Yogyakarta earthquake of May 27, 2006. Since the earthquake records on the site are not available, another way to obtain synthetic ground motions can be done in ways suggested by Bulajic and Manic (Motion records as a seismological input for seismic safety evaluation engineering structures, 2005), Rezaeian and Kiureghian (Earthq Eng Struct Dyn 39:1155–1180, 2010). Towards these ends, this research applied the Total Probability Theorem in the Seismic Hazard Probability Analysis (PSHA) with 3-D seismic sources. In this case, the PSHA analysis was carried out based on a 10% probability exceeded for 50 years building life time. The obtained uniform hazard spectrum (UHS) was then transferred to the risk targeted Maximum Credible Earthquake MCEr through the directivity factor D_f and risk targeted factor R_f with an average increase of 8.13% to UHS. Three earthquake records were selected, and after spectral matching, the high ranging bedrock

accelerations were obtained from 0.254 to 0.289 g. After conducting site response analysis, peak ground accelerations on the ground surface varied from 0.398 to 0.412 g. Furthermore, acceleration site amplifications between 1.401 and 1.426 were obtained, which are higher than the spectral site amplification between 1.215 and 1.385. Since the site amplification is still in the normal category, building damage is mostly caused by relatively high levels of ground acceleration and shaking to relatively old buildings with low material and construction quality. Although the study is still in its early stages, there are indications of fling effects on the site even though the intensity is relatively small.

Keywords Ground motions · Housing damage · Near source · Probabilistic seismic hazard analysis · Uniform hazard spectrum · Site amplification · Directivity and fling effects

1 Introduction

Although the Yogyakarta Earthquake, which occurred on May 27, 2006, took place 14 years ago, events and their impacts are still felt today. This is due to the large number of human fatalities, i.e. more than 5,500 people and more than 150,000 houses collapsed (Bappenas 2006), having especially significant impacts on the Pleret Sub-District, which is chosen as the research area. According to statistical

W. Pawirodikromo (✉)
Department of Civil Engineering, Faculty of Civil
Engineering and Planning, Islamic University
of Indonesia, Yogyakarta, Indonesia
e-mail: widodo355@gmail.com

data published by the Regional Agency of Disaster Management in Yogyakarta, of the 11,991 houses in Pleret Sub-district, only 1% were undamaged, and 12% were slightly damaged. Meanwhile, the remaining 19% were heavily damaged, and 68% experienced total collapsed. Furthermore, according to the Statistics Agency, the population density in the Special Region of Yogyakarta is categorised as very dense, resulting in a high degree of fatalities. The soil deposits in Bantul Regency are relatively thick, with a maximum depth of 145 m (Daryono 2011) so site effects cannot be avoided (Widodo 2018). Deep soil deposits and site effects, which are represented by site amplification, have been observed in many catastrophic earthquakes (Akram et al. 2017). Surface acceleration used in earthquake resistant design of buildings is a product between ground acceleration at the bedrock level and site amplification. Thus, these two aspects shape the important overarching issues that this paper seeks to examine.

Site amplification in general can be determined in two ways, namely through the motion ratio on the surface layer and outcrop, and as a ratio of motion between the surface layer with the bedrock through vertical seismic shear wave propagation (Kukusho and Sato 2008). Amplification can be determined in the form of peak to peak acceleration amplification or through spectrum amplification. The first method is very practical if the records in the two places are available. However, this is not necessarily available, especially in Indonesia. A second alternative can be pursued, however, this method also requires sediment soil data including the number and thickness of the layers and all soil properties. This is necessary to determine the stiffness of the soil layers. Spectral acceleration amplification is affected by site frequencies f_0 or site fundamentals period T (Shiuly et al. 2014), which means they are affected by the depth of the soil deposit, soil type, and property. It has been identified by researchers that at near source/field, the soil is expected to behave in-elastically so that the site amplification will be smaller as compared to far field (Kumar et al. 2015).

The near source can also be interpreted as near field earthquakes. There are no exact definitions on near source earthquake criteria, which are sometimes based on distance, while others are based on earthquake impacts expressed in Modified Mercalli Intensity I_{mm} . Kalkan and Gulkan (2004), for example,

define that near source is when an earthquake is recorded at a distance of < 15 km. Meanwhile, Stewart et al. (2001) propose the term close distance, which is the distance of the recording < 20 km. On the other hand, Maniatakis et al. (2008) explain that near source is if the region experiences an earthquake intensity of $I_{mm} \geq VIII$. The chosen site for this analysis is SMKN I Wonokromo, which is located in Pleret sub-district in Bantul Regency. The site is very close to the Opak river fault (see Fig. 2) and the distance is < 15 – 20 km from the 2006 Yogyakarta earthquake epicenter. In addition, the intensity of the earthquake in Pleret District $I_{mm} = IX$ (Widodo 2018), so that all criteria have been met that SMKN I Wonokromo falls in the near field or near source category.

The pattern of building damage due to the 2006 Yogyakarta earthquake was presented by Nurwihastuti et al. (2014), and explains that the distribution of damage is related to soil geomorphology, concluding that building damage occurs on relatively thick soil deposits. This research is semi quantitative, however, and quantitative ground acceleration and site amplification are not included in the research. Research on PGA estimation in Yogyakarta Special Province (YSP) including in Bantul Regency has also been carried out by Widodo (2018), which applied a method of PGA between YOGI and BJI stations and then extrapolated using 4-ground motion Prediction Equations (GMPE) to all of the data points at the YSP area. The results showed that the PGA in Pleret Sub-district was around 0.45 g. However, the estimated ground acceleration was derived from earthquake intensity, not from the site response analysis, and so the site amplification was not detected. Study of site amplification especially in the Opak river valley has been carried out by Perdhana and Nurchahya (2019). The Horizontal to Vertical Spectral Ratio (HVSr) method was used and results showed that the amplification factor A_f in the Pleret Valley reaches around $A_f = 7.0$. Amplification of HVSr signals in general is much higher than amplification of the results of site response analysis (Stanko et al. 2019).

Besides being located at the near source, Pleret sub-district, especially the selected site at SMKN I Wonokromo, is also located in a relatively deep sedimentary soil deposit. The data based on SPT-N field tests indicate that the elevation of hard soils is at a depth of 24 m (Widodo 2020). Considering this deep soil sedimentary deposit located near the source

corresponding with a very high percentage of residential damage in the past, therefore, it is very important to further examine the following research question(s): what is the main cause of high building damaged on site? Is it due to surface ground acceleration, soil amplification, or both?

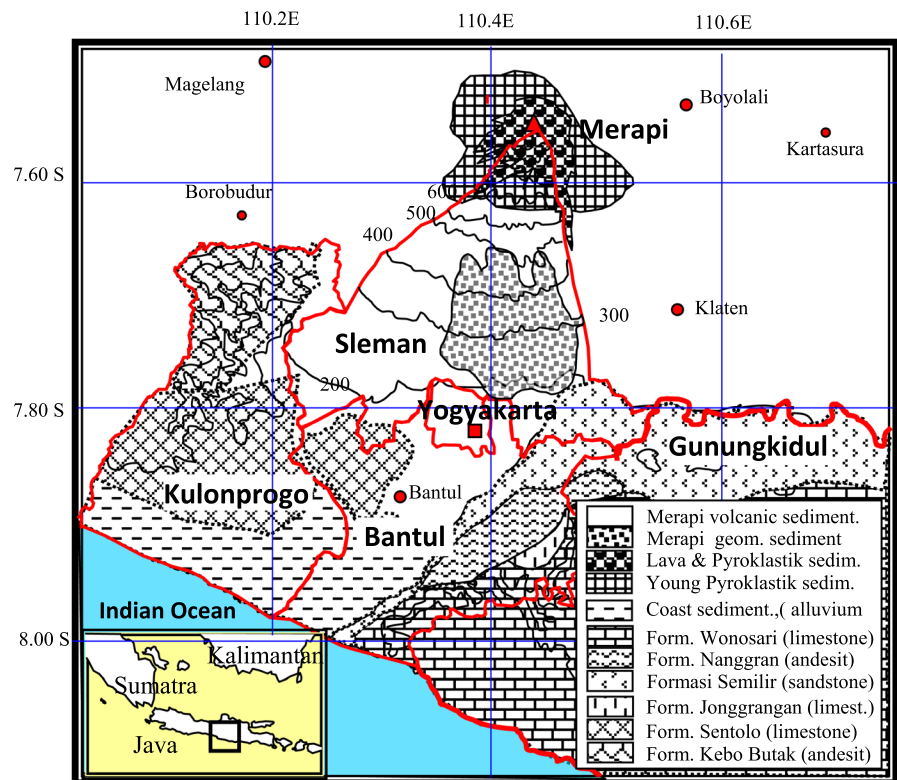
2 The Geology of the Yogyakarta Special Province (YSP)

The Yogyakarta Special Province (YSP) is located in the southern part of the province of Central Java as presented in Box insert in Fig. 1. At the north end of YSP there is an active volcano, Mount Merapi, with an altitude of 2,930 m from the sea level that last erupted in 2010. Tectonically, there is a collision between the Australian plate and the Eurasian plate at a distance of approximately 325 km south of the coast of Yogyakarta. After the Yogyakarta earthquake of May 27, 2006, an Opak river fault was identified which was only about 10 km southeast of the city of Yogyakarta. Thus, in the YSP region there are two

threats of natural disasters, namely from an eruption of mount Merapi from the northern direction and an earthquake from the southern direction. In the administrative city of Yogyakarta, there are 4 districts, namely Sleman, Gunung Kidul, Bantul and Kulonprogo, as shown in Fig. 1.

Generally, the rocks and soil in YSP consist of 3 formations (Widodo et al. 2019), namely the old rock formation, the old Merapi eruptions, and the young Merapi sedimentations (Kyaw et al. 2014). The old rock formation mainly occurs in Gunungkidul and the north-western part of Kulonprogo districts, which took place during the Tertiary period. Sleman is one of the regencies in the northern part of YSP, which is located on the slopes of Mount Merapi. Meanwhile, Bantul district is located in the southern part of the YSP, directly adjacent to the Indian Ocean. In the Quaternary period, formation/sedimentation of old, young gravel, and coarse sand occurred in Sleman and Yogyakarta city as a result of the eruptions of Mount Merapi. Most of Bantul and the southern part of Kulonprogo District are sedimentary soil formations. Their soil deposits are made up of fine sand,

Fig. 1 The local geology of Yogyakarta Special Province (YSP)



clay, and silt as a result of Tertiary sedimentary rock weathering (Nurwihastuti et al. 2014). The results of research by Daryono (2011) show that the soil in Bantul district is thick in sediment which has a high seismic vulnerability index.

Bantul district does not only consists of deep soil deposits but is also directly adjacent to the Opak river fault. The results of research on site frequency by Daryono (2011) are presented in Fig. 2. The figure shows that the small site frequency f_0 or large site period T is located on the western side parallel to the Opak river fault. That location is an area where there has been major damage and human casualties during the Yogyakarta earthquake on May 27, 2006. Figure 2 also shows the location of SMKN 1 Wonokromo, Pleret Sub-district, which is the site that has been identified as the key object of this study. The picture shows that the location of the study site is very close to the Opak river fault, only about 10 km from the epicenter of the 2006 Yogyakarta earthquake. It can be seen in Fig. 2 that SMKN 1 Pleret is only approximately 2 km from the Opak river fault.

3 Probabilistic Seismic Hazard Analysis (PSHA)

If complete earthquake recordings were available, the study of amplification and directivity effects on a site can be done relatively easily. However, such conditions are not always available in most of Indonesia, particularly at YSP. For this reason, it is necessary to find a solution as proposed by Bulajic and Manic (2005) and Rezaeian and Kiureghian (2010), whereby synthetic ground motion (SGM) can be generated with combined stochastic, deterministic, and probabilistic approaches. In this study the Probabilistic Seismic Hazard Analysis (PSHA) method is based on the Total Probability Theorem. The PSHA analysis is required primarily to determine synthetic ground acceleration at bedrock levels.

After being introduced by Cornell (1978), the PSHA method has developed rapidly and has come to be a common method for conducting a routine calculation. Step-by step of the PSHA calculation

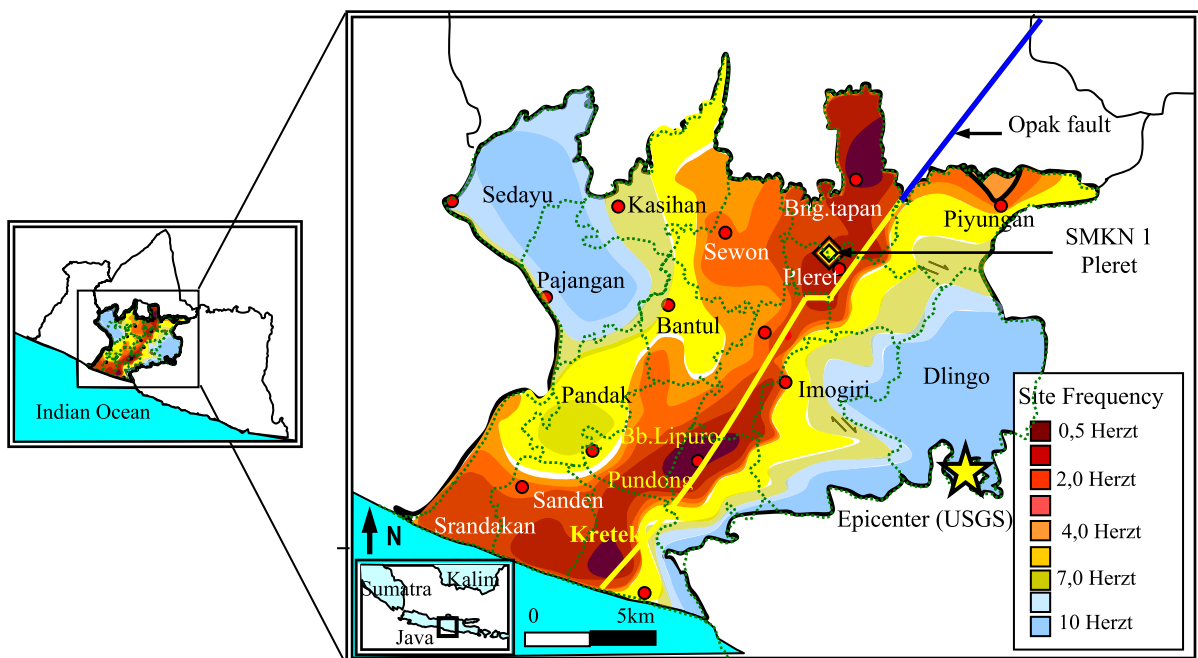


Fig. 2 Site frequency at the Bantul Regency (Daryono 2011) and location of SMKN 1 Pleret

procedures are proposed in Baker (2008). In the total probability theorem, the annual rate of exceedance $\lambda(IM > x)$ at specified ground motion amplitudes (for example for ground acceleration) can be determined through the formula (Atkinson 2004),

$$\lambda(IM > x) = \sum_{i=1}^n \nu(M > m_{\min}) \iint P(IM > x | m, r) f_M(m) f_R(r) dr dm \quad (1)$$

where $\nu(M > m_{\min})$ is the annual earthquake rate of occurrence greater than the minimum magnitude m_{\min} , $P(IM > x | m, r)$, which is the probability of intensity measure IM that is greater than x caused by variables earthquake magnitude m and distance r , F_M and F_R , respectively, are a cumulative probability function of m and r .

The annual rate of exceedance as presented in Eq. 1 is calculated based on the pseudo-spectral acceleration (PSA) for a given T vibration period, so that a hazard curve can be made for each desired T period. Based on the hazard curve, then Uniform Hazard Spectrum (UHS) can be developed for each annual rate of exceedance under consideration. Thus, the bed-rock, short period, and long period hazard map can be established. Complete formulation and PSHA analysis procedures can be found in many research publications.

4 Near Source Spectral Demand, Directivity and Fling Effects

Earthquakes are generally recorded in a 3-axis formulation, the x -direction, y direction and z direction (vertical). Records in the x -direction and the y -direction generally have different PGAs, especially for sites that are very close to faults where directivity effects may occur (Yahyai et al. 2011; Bradley and, Baker 2014). The consequences of seismic near field domains on the structures have been discussed by Grimaz and Malisan (2014), which highlight the effects of: (1) vertical acceleration; (2) hinging wall; (3) directivity; (4) fling-step; (5) velocity pulse and (6) rotational seismic component. In the Indonesian seismic code, not all effects have been taken into account, only the vertical and directivity effects.

Directivity effects will occur if the fault rupture velocity is very close to the shear wave velocity in the media. In the forward directivity, the PGA in the fault-normal direction can be much greater with a longer period velocity pulse-like dimension than the fault-parallel (Gerami and Abdollahzadeh 2012). The geometric mean spectral level is generally used in the PSHA (Huang et al. 2008), where its value is determined by only the square-roots of the product between the spectral in x -direction and y -directions, accordingly, and the directivity effects should be taken into account. However, sometimes it used the biggest spectral between 2-direction records (Bradley and Baker 2014; Boore 2010). Fling effects also occur in the near source site which is indicated by the presence of non-zero ground displacement at the end of the record (Kamai and Abrahamson 2015).

In the 2019 Indonesian Seismic Design Code, the directivity effect has been considered by applying directivity factor D_f . This D_f factor is intended to connect between geometric mean spectrum and spectral acceleration at Maximum Credible Earthquake (MCE), where the D_f is the function of the period T (Fema p-1050 2015). The directivity factor for $T=0$ s can be taken $D_f=1$, for the period $T=0.2$ s the value of $D_f=1.1$ and for the period $T=1.0$ s, the value of the directivity factor $D_f=1.3$. From $T=0$ s to $T=0.2$ s and from $T=0.2$ s to $T=1.0$ s, the D_f value can be calculated linearly. For $T > 1.0$ s, the directivity factor is constant, $D_f=1.3$ (Sengara and Komerdevi 2019).

It is necessary to also express that at the MCE level, it cannot guarantee the occurrence of building collapse during 50 years (Fema p-1050 2015) with the same risk. Therefore, in order for the uniform risk to occur, the risk targeted coefficient factor, R_f should be taken into account. The ground motions will then reach the Risk Targeted Maximum Credible earthquake MCEr. Based on the Indonesian Seismic Code, the risk targeted coefficient has been presented in the form of a map that is C_{RS} map for short period $T=0.2$ s and C_{R1} map for the long period $T=1.0$ s.

5 Vertical Seismic Shear Wave Propagation

The propagation of earthquake waves from bedrock to the ground surface is usually done by assuming

that the shear waves propagate vertically. Wave propagation can be modeled as 1-D, 2-D or even 3-D which are relatively complex. Because of its complexity, 2-D and 3-D wave propagation models are still rarely used, so it is generally modeled as 1-D. Meanwhile the response of soil media can be considered as equivalent linear or non-linear. On the other hand, layered soil media can be modeled as discrete or continuous models. If soil media is modeled discretely, then the differential equation of ground mass movement due to base motions can be written as (Presti et al. 2006),

$$M \frac{d^2 Y}{dt^2} + C \frac{dY}{dt} + K.Y = -Mr.\ddot{y}_b \quad (2)$$

In which M, C and K, respectively, are, mass, damping and stiffness matrices, Y is horizontal displacement, r is scalar vector and \ddot{y}_b is base motions.

If a continuous model is used, the partial differential equation of mass motion is (Park and Hashash 2004),

$$\rho \frac{d^2 y}{dt^2} = G \frac{d^2 y}{dz^2} + \eta \frac{d^3 y}{dz^2 dt} \quad (3)$$

In which ρ is mass density of media, y is horizontal displacement, z is soil depth, G is soils shear modulus and η is viscosity.

The numerical solution Eq. 3) has been presented by Bardet et al. (2001) as well as through

the Computer Package Program NERA (Nonlinear Earthquake Site Response Analysis).

6 Method of Investigation

6.1 Earthquake Data

The seismic source mechanism identified for the YSP is subduction (Megathrust and Benioff) and shallow crustal earthquakes. Earthquake data for both subduction and shallow crustal events from 1963 to 2017 occurred within a radius of 500 km from the city of Yogyakarta as shown in Fig. 3 were considered in this study. The earthquake data was taken from earthquakes with magnitudes greater than M5.0, with a depth of less than 700 km. The earthquake data was downloaded from the USGS catalog. A Computer Program for PSHA called the SHModel (Makrup 2009) was used. In this software, PSHA was conducted based on the Total Probability Theorem with 3-D earthquake sources.

6.2 Earthquake source identification

6.2.1 Shallow Crustal Earthquake sources

Sources of shallow crustal earthquakes that are still within a radius of 500 km from Yogyakarta are:

(1) West Java (Cimandiri, Lembang, Baribis and

Fig. 3 The earthquake source mechanism of the YSP

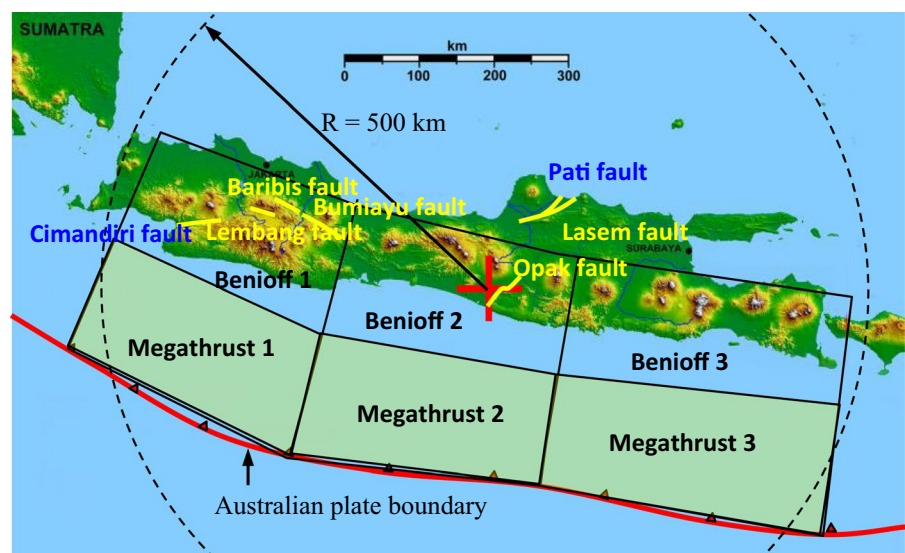


Table 1 The data and parameter fault in Yogyakarta and Central Java

No	Fault	Slip-rate	Source mech	Fault length	a	b	Rate v	Dip	M _{max}
1	Opak	2.4 mm/y	rstrike-slip	31.6 km	2.985	1	0.010	90	6.8
2	Lasem	0.5 mm/y	Strike -slip	114.9 km	3.389	1	0.021	90	6.6
3	Pati	0.5 mm/y	Strike slip	51.4 km	3.383	1	0.024	90	6.8
4	Bumiayu	0.5 mm/y	strike-slip	44 km	2.985	1	0.010	90	6.0
5	Cimandiri	2.0 mm/y	Strike-slip	98 km	4.057	1	0.114	90	7.2
6	Baribis	0.2 mm/y	Strike-slip	64 km	2.985	1	0.010	90	6,8
7	Lembang	2.0 mm/y	Strike-slip	30 km	3.949	1	0.089	90	6.6

Table 2 Source model of Subduction earthquake mechanism

No	Source Model	Zone								
		Megathrust-1			Megathrust-2			Megathrust-3		
		a	b	Rate v	a	b	Rate v	a	b	Rate v
1	Megathrust	6.14	1.10	4.365	6.14	1.10	4.365	6.14	1.10	4.365
		Benioff-1			Benioff-2			Benioff-3		
2	Benioff	5.54	1.08	1.38	6.04	1.19	1.23	7.10	1.40	1.259

Bumiayu); (2) Central Java (Pati, Lasem) and (3) Yogyakarta (Opak). Based on the data, source mechanism, slip rate, fault length, dip angle, magnitude M and computed a and b are presented in Tables 1 and 2 (Febriani 2015; Nguyen et al. 2015; Sunardi 2016; Irsyam et al. 2017; Partono et al. 2017).

6.2.2 Megathrust source mechanism

Another earthquake source mechanism that must be considered in YSP is caused by the subduction of the Australian plate with respect to the Eurasian plate. As shown in Fig. 3) and Table 2, within a 500 km radius of the city of Yogyakarta, the subduction earthquake source was divided into 3 zones i.e. zone-1, zone-2, and zone-3. Each zone consists of Megathrust and Benioff earthquake sources. According to Daryono (2011), subduction activity in the south of the island of Java has a potential to cause a maximum earthquake of Mw8.1.

6.3 The Ground Motion Prediction Equation (GMPE) and Logic Tree

The general and detailed criteria for selecting and adjusting the GMPE models have been presented briefly by Cotton et al. (2006), Douglas et al. (2009). Among the general criteria is to consider

global earthquake models and exclusion criteria (Cotton et al. 2006; Bommer et al. 2010; Stewart et al. 2015). Considering that GMPE is not available, then the GMPEs from other countries are used i.e. those developed by Sadigh et al. (1997) and Boore and Atkinson (2007) for shallow crustal processes and Chiou and Young (2006) and Atkinson and Boore (2006) for Megathrust & Benioff sources.

The researchers agree that there are intrinsic uncertainties and aleatory uncertainty (Strasser et al. 2008; Bommer et al. 2010; Atkinson 2011) in the PSHA. The epistemic uncertainty can be treated by applying the logic tree model (Foulser-Piggott 2014), meanwhile, aleatory uncertainty is usually treated by applying the standard deviation or sigma (Cotton et al. 2006). Because of the degree of uncertainty, the weighting factor for each GMPE is commonly used. The GMPE candidate and weighting factor are assessed through expert judgment and tested through procedures such as presented by Delavaud et al. (2012). Depends on the GMPE used, the logic tree for shallow crustal earthquake source is presented in Fig. 4), while for Megathrust and Benioff is presented in Fig. 5).

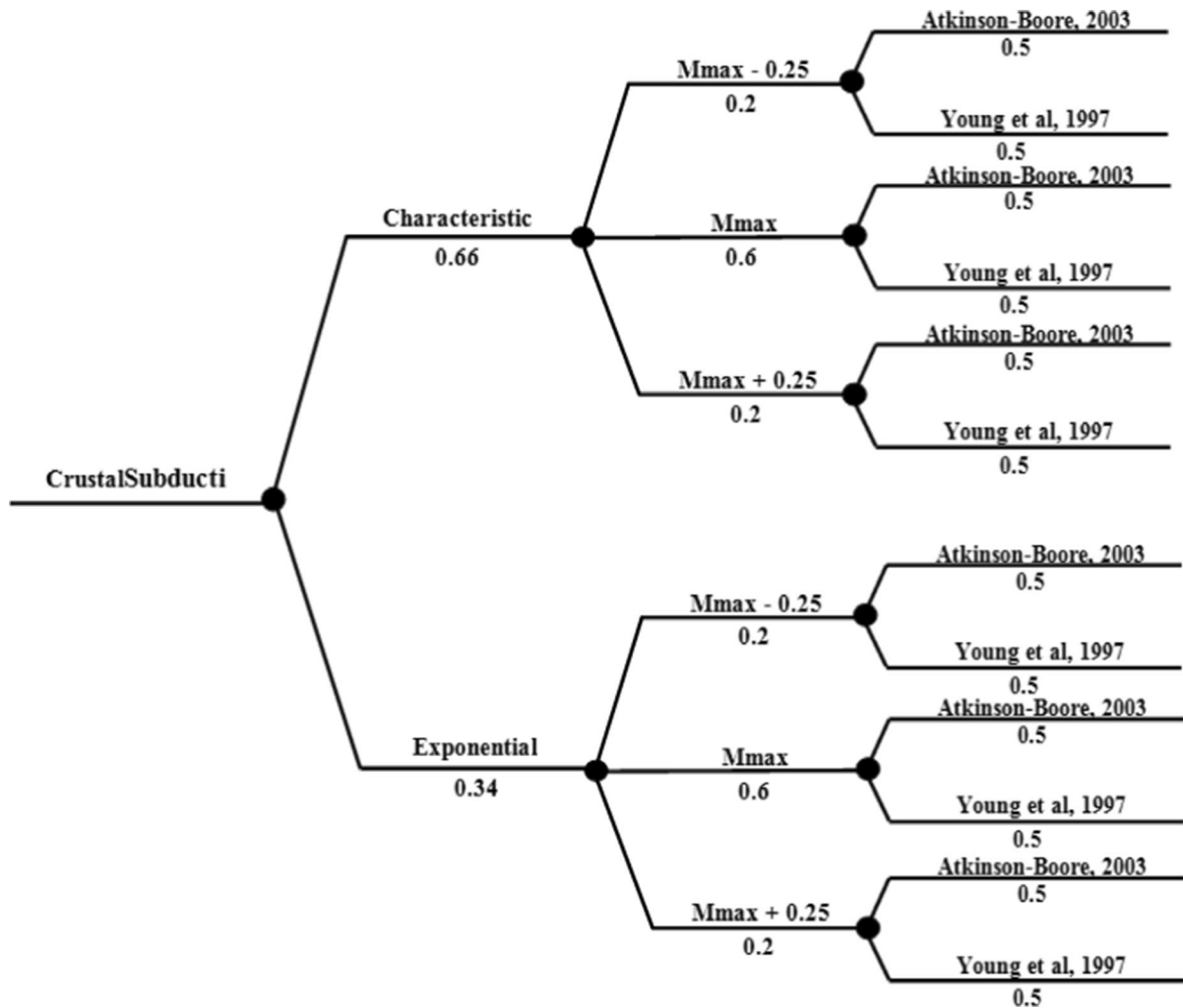


Fig. 4 Logic tree for Megathrust Benioff and source mechanism (Makrup, 2009)

7 Results and Discussion

7.1 Site Classification and Shear Modulus Reduction Curve

This research is a combination between field and simulation studies. Field research included data collection of soil layers in terms of number, layer thickness, and depth of hard soils. In addition to these data, soil physical property and SPT-N field tests data are also required. The number of layers, types of soil layers, and SPT-N field test results are as presented in Fig. 6a).

In Fig. 6a it appears that the average SPT-N in the upper 24 m layer is $N=40.1$. According to the

Indonesian Seismic Loading Code SNI 1726, 2019 the site is categorized as medium soil. The calculated shear wave velocity V_{S30} and the maximum soil shear modulus G_0 for each layer are as presented in Fig. 6b, c. Due to the unavailability of complete soil data, V_{S30} was computed based on: (a) Imai (1977) for sands; (b) Hasancebi and Ulusay (2006) for all soils, and G_0 are calculated based on: (a) Ohta et al. (1972) for sandy soil; (b) Hara et al. (1974) for alluvial soils. All empirical formulas for V_{S30} and G_0 are adopted from Anbazhagan et al. (2012) and Bandyopadhyay et al. (2019). As shown in the picture, the average shear wave velocity at the 30 m upper layer is $V_{S30}=278.95$ m/s. Based on the Indonesian Seismic

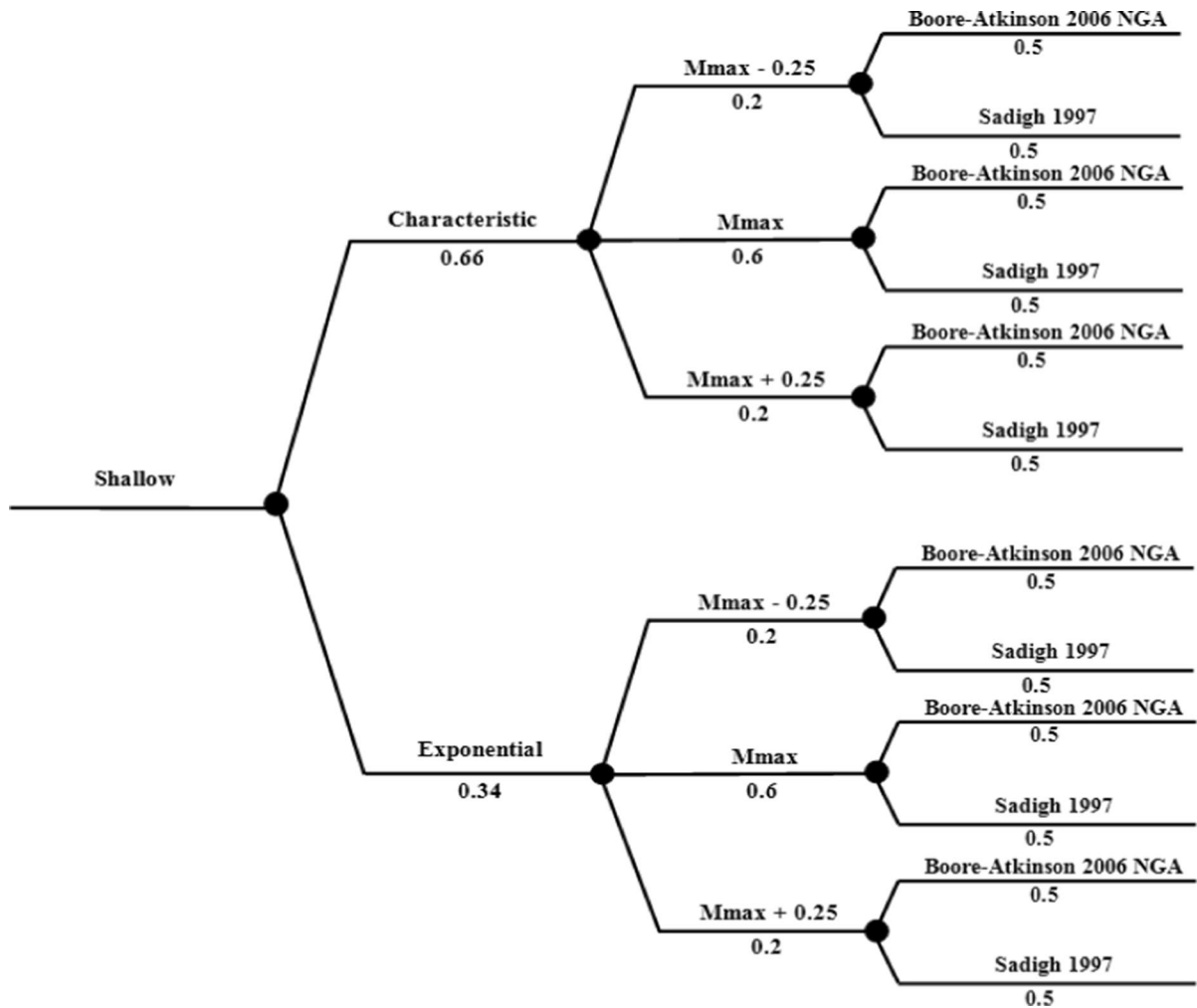


Fig. 5 Logic tree for shallow crustal source mechanism (Makrup, 2009)

Loading Code SNI 1726,2019 the site falls into the medium soil category, similar as the previous result.

In Fig. 6a shows that the 2-top soil layers are fine sandy loam. Based on laboratory tests, the soil layer has plasticity index of $PI=26.66\%$. The following two-layers below, consists of sand layers (with assumed $PI=0-5\%$) and the next 2-layers below is fine sandy loam with $PI=18.86\%$. Based on the soil physical properties, the ratios of shear modulus reduction G/G_0 and damping curves D/D_{max} are as presented in Fig. 7. These curves will be used to determine the stiffness and damping of the soil layer which are a function of its soil shear strain (Fig. 8). The similar soil category is also obtained based on the site period T as presented in Fig. 8. Average site period

in Pleret District is $T=0.492$ s. Meanwhile based on the value of shear modulus of each layer, the value of site period $T=0.43$ s is obtained. According to the soil type categorizations presented by Ji et al. (2017) the site also falls in the medium soil category.

7.2 The Hazard Curve of the Site

The hazard curve is the relationship between ground acceleration (g) and annual rate of exceedance. The hazard curve for the SMKN-1 Pleret site is presented in Fig. 9. The figure shows that the acceleration at $T=0.20$ s is the largest in the entire spectral period T . In the period $T < 0.2$ s and $T > 0.2$ s, the acceleration values will decrease. The UHS of the site will

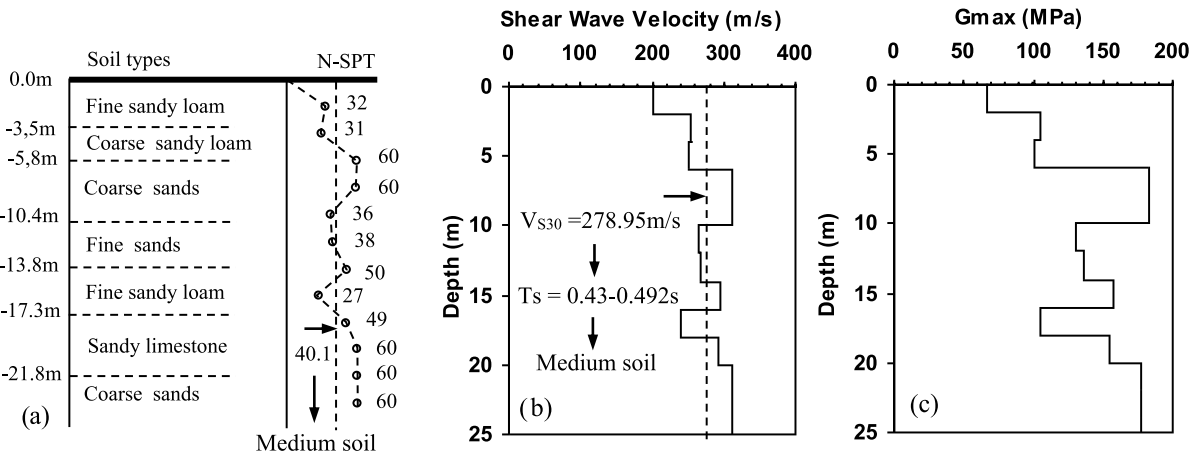


Fig. 6 Soil profile; a Maximum Shear Modulus Gmax; b Shear Wave Velocity, Vs

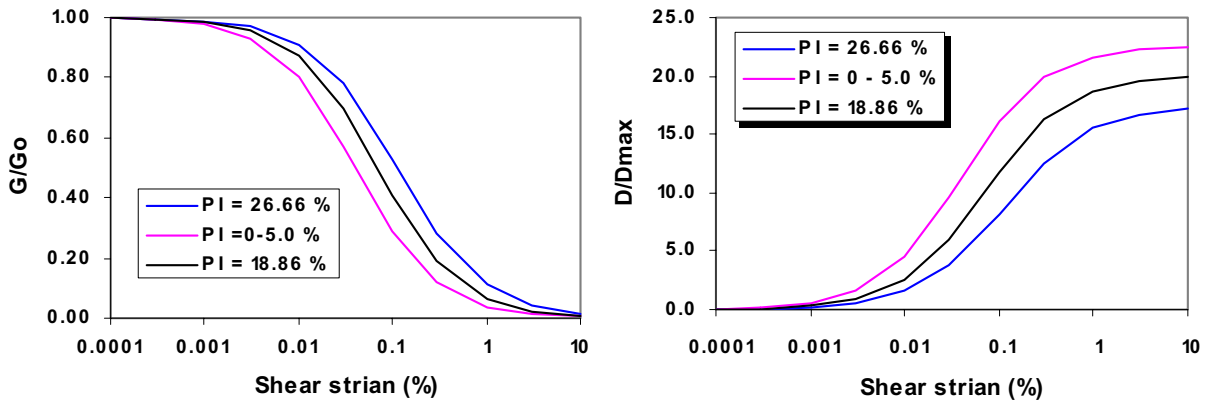


Fig. 7 Shear Modulus Reduction and Damping Curves

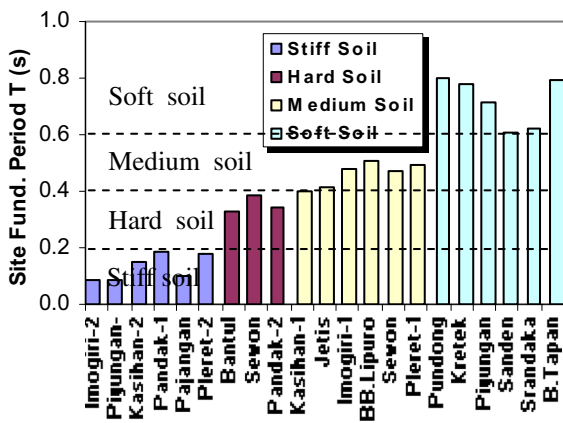


Fig. 8 Site Period T of the sub-Districts in Bantul

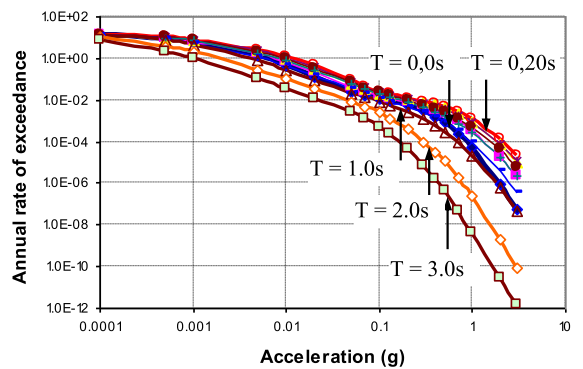


Fig. 9 Hazard Curve at SMKN 1 Pleret YSP

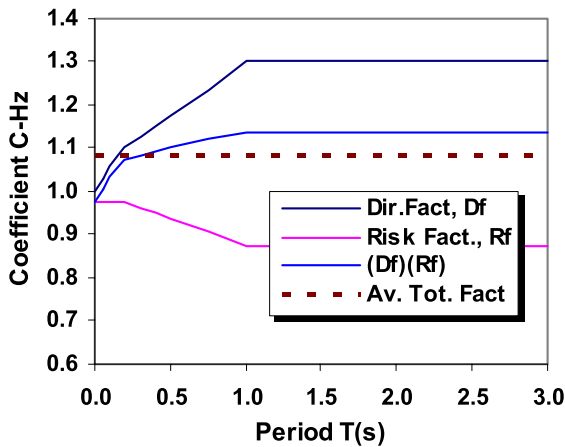


Fig. 10 Directivity and risk targeted factors

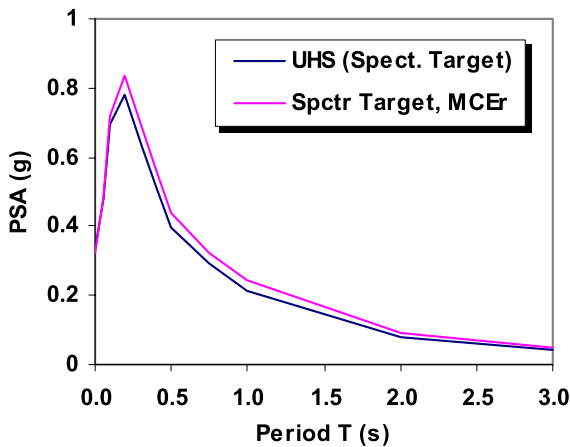


Fig. 11 UHS and spectra target MCEr

be obtained by considering a particular annual rate of exceedance. The spectrum is called to be uniform because it is developed at the same annual rate of exceedance.

7.3 The UHS targeted spectra MCEr

Figure 11 is a UHS for SMKN-1 Pleret developed from a hazard curve as presented in Fig. 9. The computed peak UHS at SMKN-1 Pleret is very high. This result is the first finding of this study. This result is about 60% higher than the result as reported by Sunardi (2016) i.e. for the site at 15 km from the Opak river fault or 25 km from the epicenter of

the 2006 Yogyakarta earthquake. This is because as mentioned before, the location of SMKN-1 is only approximately 2 km away from the Opak river fault.

As previously stated, the UHS is the result of using the ground motion prediction equation (GMPE) at the mean geometric level. To develop a maximum spectrum demand at the level of maximum credible earthquake MCEr, the directivity factor D_f and the targeted R_f factor are considered. The product between D_f and T_f is risk factor R_f as presented in Fig. 10. The end result is a risk targeted spectrum at the MCEr level as shown in Fig. 11. The MCEr targeted spectrum represents a demand spectrum at the bedrock level. There was an average increase of 8.13% from the UHS geometric mean to the risk targeted response spectrum MCEr level.

7.4 Matched ground accelerations

The next step was to look for a ground acceleration record whose response spectrum matches with the MCEr spectrum demand. Considering that the local earthquake records are not available, then records from several countries needed to be used. Spectrum response in bedrock, in general, possesses high frequency content. Therefore, if a well matching spectrum is desired, the earthquakes with high frequency content are required. Finally, the Mammoth Lake (MLakeMIs2E) earthquake, Coyote Lake earthquake (ClakeGil2E) and the Friuli, Italy earthquake (FriuliFocE) were chosen. The results of matching spectrum are shown in Fig. 12. It appears in the figures that the three earthquakes match well against the MCEr spectrum demand.

7.5 Ground Motions and Amplification Factors

Based on the Indonesian Seismic Code 1726, 2019, 11-earthquake records are required for time history analysis. Because of limited space, only 3 among 11 original earthquake records are considered and presented in Fig. 13).

Figure 13 presents the maximum ground accelerations and its significant earthquake duration D_{595} . In Fig. 13, it appears that three records have significant earthquake duration of D_{595} , with 9.02 s, 15.27 s, and 10.32 s, respectively. These values of D_{595} still meet the requirements as stated by Kempton and Stewart (2006). In addition, the MLakeMIs2E earthquake has the largest integral of the square of the ground

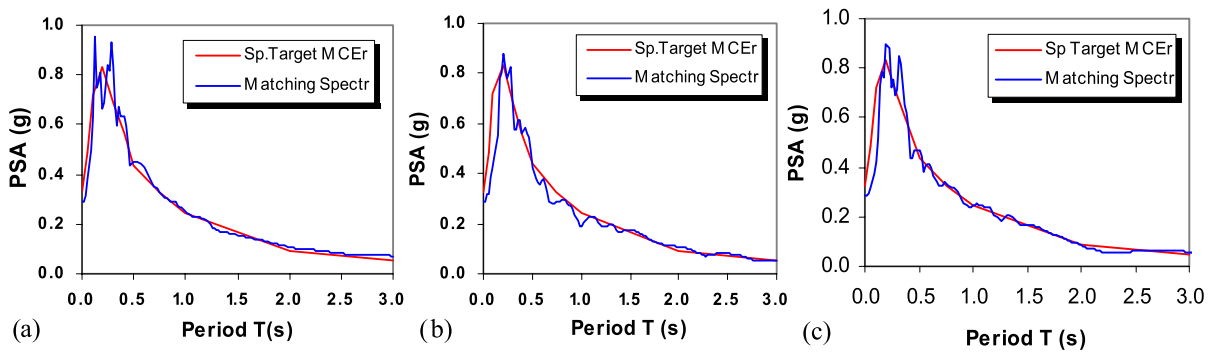


Fig. 12 Matching spectrum: a MammouthLake; b Coyote Lake; c Imp. Valley 1979 earthquakes

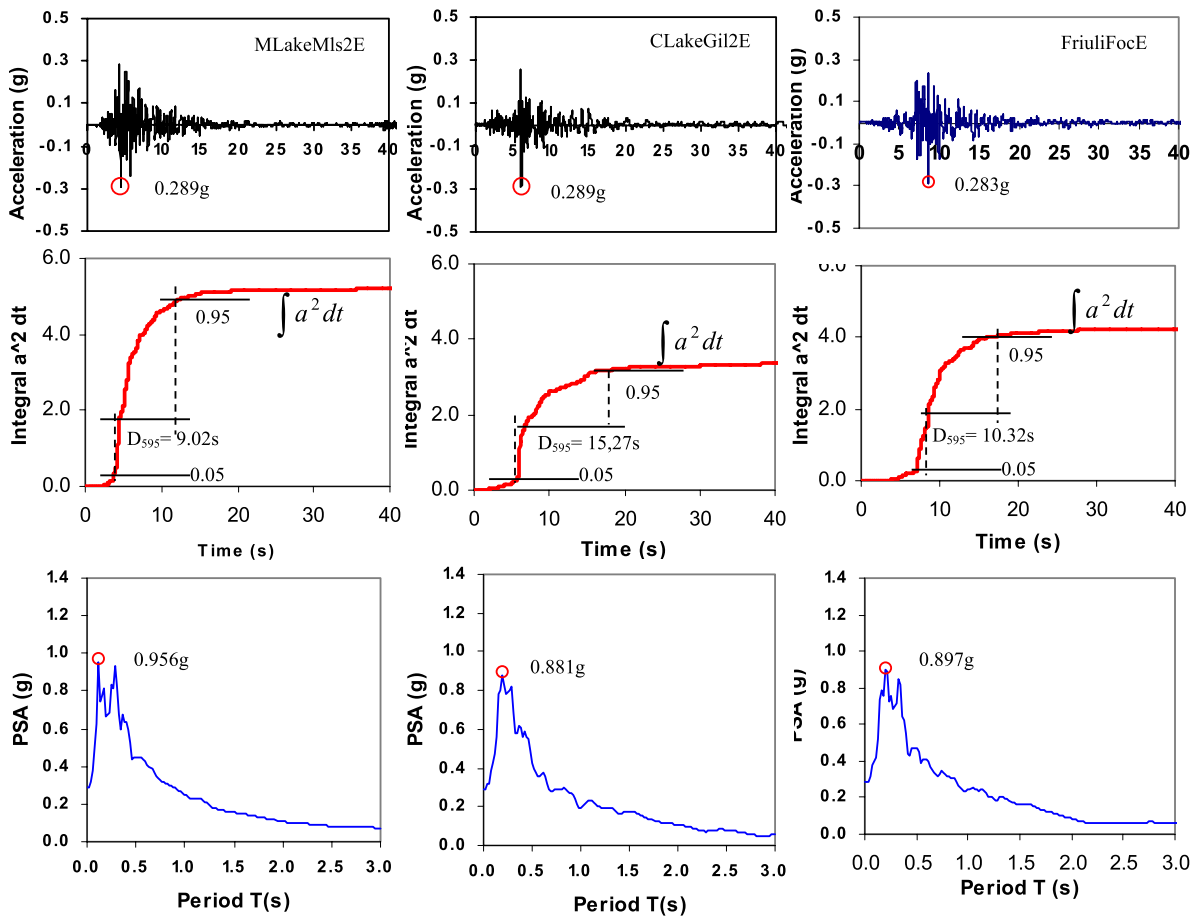


Fig. 13 Original ground acceleration, significant duration D_{595} and response spectrum

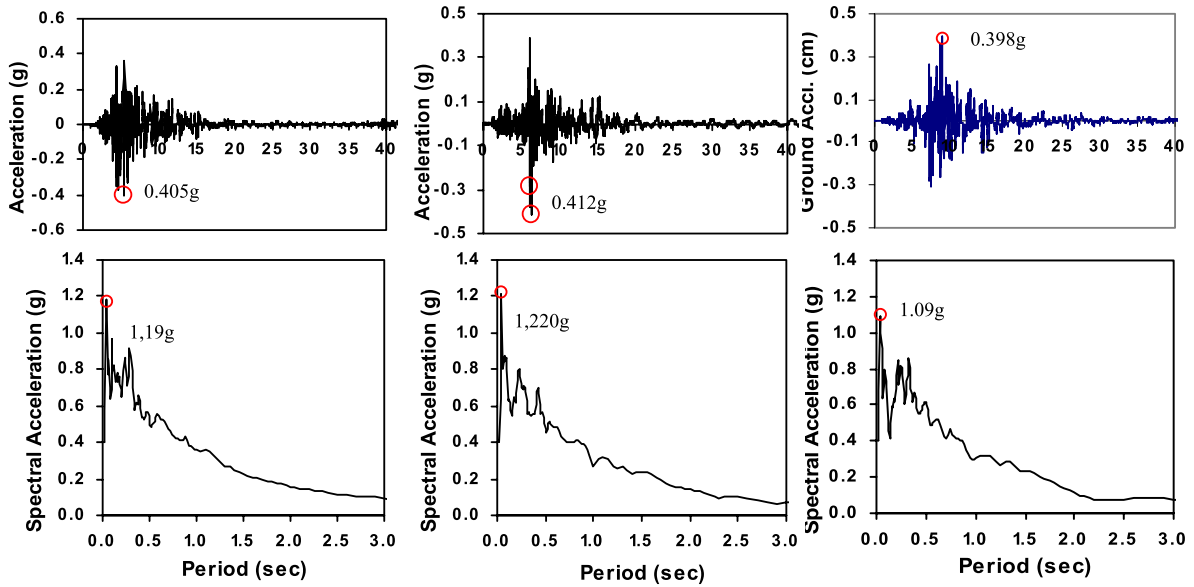


Fig. 14 Surface ground acceleration and response spectrum

acceleration, so that it has larger energy content on its ground acceleration.

Meanwhile, Fig. 14 is the ground acceleration and response spectrum at ground level resulting from vertical propagation of seismic shear waves by the NERA Computer Package Program. Based on Figs. 13 and 14 peak to peak ground acceleration and spectral amplification factors can be determined. The summary of soil amplification factors is presented in Table 3. The table shows ground acceleration amplification factor ranges from 1.401 to 1.426. Meanwhile the spectrum amplification factor is lower, ranging between 1.215–1.385. The amplification factor is relatively close to the results by Stanko et al. (2019) ranging from 1.1 to 2.0 but still lower than the amplification factor provided by Shiuly et al. (2014)

and Bandyopadhyay et al. (2019) which ranged from 1.52 to 3.84. This happens because the site period at SMK 1 Pleret is $T=0.43$ to 0.492 s (more stiff), while the site period T by Shiuly et al. (2014) ranges from $T=0.33$ to $T=0.89$ s. Since the data is limited the decrease in amplification takes place as the PGA increases Bajaj and Anbazhagan (2017) has not been observed. The result of amplifications becomes the second finding of this study. Based on the results, the site amplification factors still fall in the normal levels.

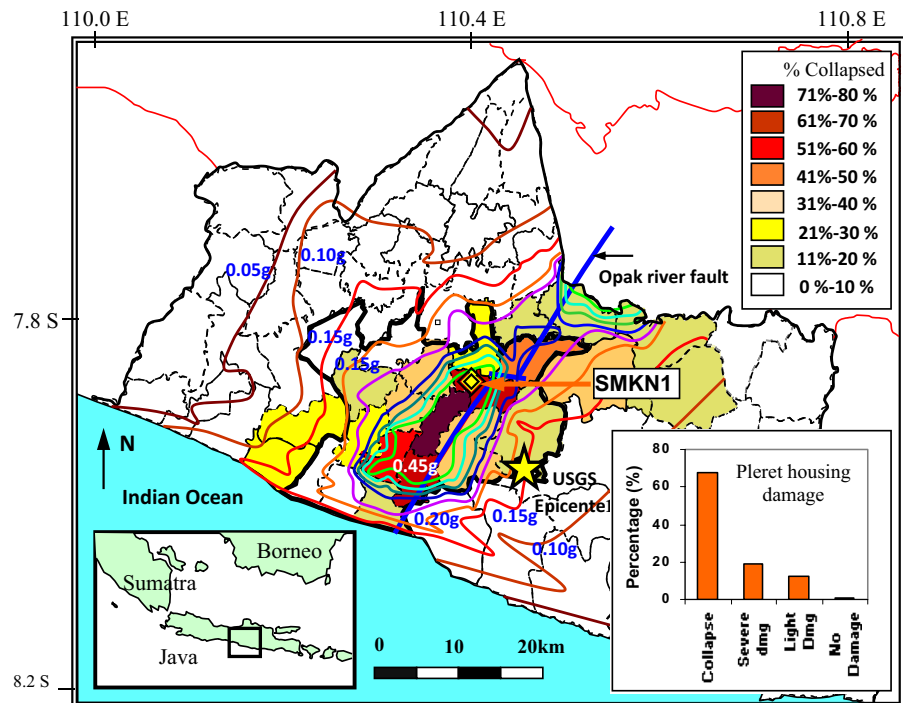
7.6 Distribution of Housing Damage

The damage to houses in Pleret sub-district was very high. Based on the Yogyakarta Regional Agency for Disaster Management (BPBD), the percentage

Table 3 Ground acceleration and spectral amplification

No	Level & Amplification	Peak ground acceleration (g) and D_{595}			Peak Response spectrum (g)		
		MLakeMIsE	ClakeGiIE	FriuliFocE	MLakeMIsE	ClakeGiIE	FriuliFocE
1	Bedrock level	0.289	0.289	0.283	0.956	0.881	0.897
	Sign. Dur., D_{595}	9.01 s	15.27 s	10.32			
2	Ground Surface	0.405	0.412	0.397	1.190	1.220	1.090
	Sign. Dur., D_{595}	10.01 s	15.69 s	11.50			
3	Amplification	1.401	1.426	1.402	1.244	1.385	1.215

Fig. 15 Map distribution of housing damage



distribution of building damage at YSP especially in Bantul Regency is shown in Fig. 15. The figure shows the percentage of building collapse in Pleret District where SMKN 1 is located, and ranks second after the Jetis sub-district site. In Jetis sub-district, 71% of houses collapsed, higher than in Pleret sub-district, where 68% houses collapsed. In the previous wave propagation process, it was found that the ground acceleration ranged from 0.393 to 0.412 g, meanwhile the result of a ground acceleration study by Widodo (2018) is 0.45 g, as shown in the figure above. It appears that the two study results are quite similar as a means of mutual verification.

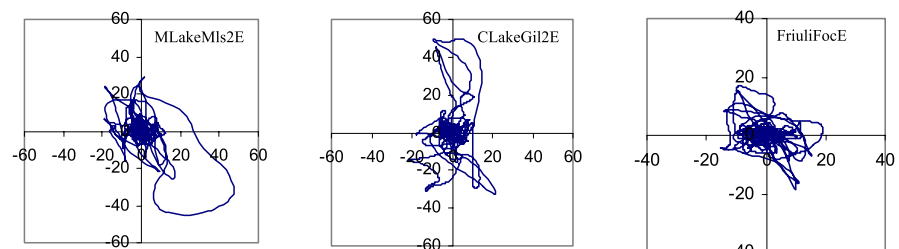
Site amplification in Pleret Sub-district results of this study is still relatively normal because it is close to the results of other researchers' studies. However,

because the Pleret District is a near source site, the ground acceleration is relatively high, reaching around 0.40 to 0.45 g. This high ground acceleration is thought to be one of the causes of high building collapse, in addition to being influenced by the quality of the building itself. Considering that the location of Pleret sub-district is near source, improving the quality of buildings is a very important action to reduce risks in the future.

7.7 Identification of the Directivity and Fling Effects in Near Source Site

Ideally, an analysis of the presence of directivity and fling-step would be better if there were earthquake records in the field. Because there was no earthquake

Fig. 16 Bidirectional velocity record



record on hand, then the analysis was only done on developed synthetic ground motion analysis. The velocity of bidirectional records of the developed synthetic ground acceleration are presented in Fig. 16. The figure shows the first 2-earthquake records and indicates directivity and fling effects. Therefore, if only geometric mean is applied in the development of PSHA spectra demand, the process will yield inaccurate results. Thus, applying directivity factor D_f in constructing spectral demand is crucial factor, because it better represents events in the field.

Meanwhile, the ground displacement time history of the three selected earthquake records is shown in Fig. 17. The MammothLake(MLakeMIs2E) and Coyote Lake(CLakeGil2E) earthquakes are interesting when compared to the others because there is a permanent ground displacement at the end of the record. Figure 17 shows the ground displacement time history on the ground surface resulting from the site response analysis. As stated by Kamai and Abrahamson (2015) this is one of the characteristics of fling effects. Although its permanent ground displacement is not very extreme and not taken from original local earthquake records as presented by Kamai and Abrahamson (2015) the fling effects in the near source site such as in Pleret sub-district must be taken into consideration and account in the seismic analysis.

8 Conclusions

This study has focused on ground acceleration, site amplification, and building damage at a near source earthquake and its dynamics at SMKN 1, located in the heavily impacted Pleret subdistrict in Yogyakarta, Indonesia.

Several criteria have been used, namely shear wave velocity V_s , site period T and SPT-N blow count values in determining the soil types. Even though the damage to the building in Pleret sub-district was large, the type of soils in the Pleret sub-district does not include soft soil types, but is still classified as an intermediate soil. The use of 3- criteria for classifying the soil type has fulfilled the requirements as written in The Indonesian Seismic Loading Code SNI 1726, 2019.

The main finding of this study is that the peak UHS spectrum demand in bedrock level is so high because of the location of the study site (SMKN 1, Pleret), which is very close to the Opak river fault. The directivity and risk targeted effects have been considered by applying the Directivity Factor D_f and the risk targeted factor R_f towards the level of risk targeted maximum credible earthquake MCEr. From the geometric mean spectrum demand to the risk targeted spectrum demand has increased on average by 8.13%. The average increase of the factors is not so large because the value of the risk targeted factor R_f on the site is less than 1.0.

Given the limited space, only 3-earthquake records, namely the Mammoth Lake earthquake (MLakeMIs2E), Coyote Lake earthquake (CLakeGil2E) and Friuli earthquake (FriuliFocE) have been selected and matched with the targeted spectrum demand at MCEr level. The significant duration D_{595} value of the selected earthquakes still meets the requirements as presented by Kempton and Stewart (2006). The peak ground acceleration (PGA) in the bedrock obtained in this study is in the range of 0.254 g to 0.289 g. This PGA value is felt to be large enough. This happens because the location of SMKN 1 in Pleret Sub-district is very close to the Opak river fault. The maximum spectrum

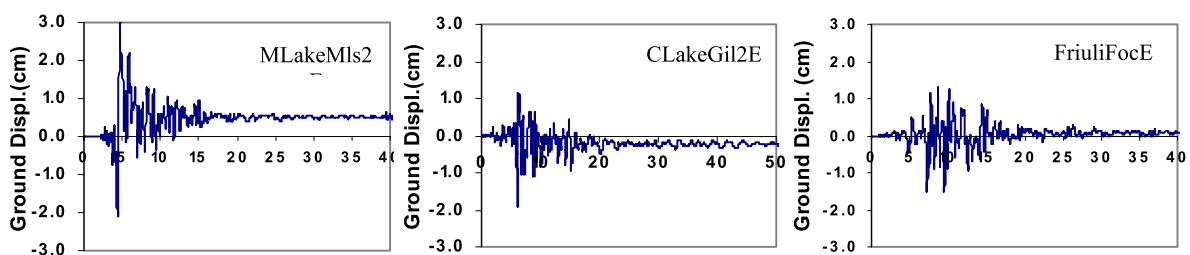


Fig. 17 Ground Displacement time history

values in the fundamental period T at the bedrock level are 0.956, 0.881 and 0.897 g, respectively.

The additional finding is that the PGA site amplifications range from 1.401 to 1.426, so that the PGA on the ground surface ranges from 0.398 to 0.412 g. This result is quite close to the estimation by Widodo (2018), that is, a PGA around 0.45 g, although that study applied different methods. Meanwhile, the peak response spectrum on the ground surface ranges from 1.09 to 1.22 g so that the site amplification spectrum ranges from 1.215 to 1.285. Site spectrum amplification is smaller than site acceleration amplification and these results are comparable to those presented by Stanko et al. (2019). Statistics for damages to housing in Pleret come only second after Jetis Sub-District. If the site amplification is still in the normal category, the building damage is mostly caused by relatively high ground acceleration. This has become the main finding of this study. In addition to high ground acceleration, housing damage is also aggravated by the presence of older buildings, low quality of material, and poor construction methods (Bappenas 2006).

Identification of directivity effects has been carried out. Although the earthquakes used in this study are not from the original records from the site, however, the effect of directivity effects has been taken into account in determining the spectrum of the risk targeted Maximum Credible earthquake MCEr. Furthermore, although this analysis is still in the initial stage, identification of the possibility of fling effects has also been carried out. There are indications that fling effects may occur in the site even though they are still relatively small. This is indicated by the presence of permanent ground displacements at the end of the record at ground level as stated by Kamai and Abrahamson (2015). The fling effects have not been taken into account in the Indonesian Seismic Design Code 2019.

Funding The authors have not disclosed any funding.

Data availability Enquiries about data availability should be directed to the authors.

Declarations

Competing interests The authors have not disclosed any competing interests.

References

- Akram MR, Yesilyurt A, Zulfikar AC (2017) Site amplification and response analysis: a case study of October 6th 2000, M7.3 Western Tottori Earthquake Japan. In: 4th international conference on earthquake engineering and seismology, Anadolu University Turkey
- Anbazhagan P, Parihar A, Rashmi HN (2012) Review of correlation between SPT-N and shear modulus: a new correlation applicable to any region. *Soil Dyn Earthq Eng* 36:52–69
- Atkinson GM (2004) An overview of the development of seismic hazard analysis. In: 13th World conference on earthquake engineering, Vancouver, Canada, Paper No.5001
- Atkinson GM (2011) An empirical perspective on uncertainty in earthquake ground motion prediction. *Can J Civ Eng* 38(9):1002–1015
- Atkinson GM, Boore DM (2006) Earthquake ground-motion prediction equations for Eastern North America. *Bulletin Seismol Soc America* 96(6):2181–2205
- Bajaj K, Anbazhagan P (2017) Ground motion site amplification factors for deep soil deposits sites Indo-Gangetic Basin, PBD III, Earthquake Geotechnical Engineering, Vancouver Canada.
- Baker JW (2008) An introduction probabilistic seismic hazard analysis (PSHA). Stanford University, Version 1.3, 72 p.
- Bandyopadhyay S, Sengupta A, Reddy GR (2019) Development of correlation between SPT-N value and shear wave velocity and estimation of nonlinear seismic site effects for soft deposits in Kolkata city. *Geomech Geoeng Int J* 1–19
- Bappenas (2006) Preliminary damage and loss assessment Yogyakarta and Central Java Natural Disaster, The Consultative Group on Indonesia, p 140
- Bardet JP, Tobita T, NERA (2001) A computer program for nonlinear earthquake site response analysis of layered soil deposits. Department of Civil Engineering, University of Southern California, p 44
- Bommer JJ, Douglas J, Scherbaum F, Cotton F, Bungum H, Fah D (2010) On the selection of ground-motion prediction equations for seismic hazard analysis. *Seismol Res Lett* 81(5):783–793
- Boore DM (2010) Orientation-Independent, Nongeometric-Mean Measures of Seismic Intensity from Two Horizontal Components of Motion. *Bull Seismol Soc Am* 10(4):1830–1835
- Boore DM, Atkinson GM (2007) Ground motion relations for geometric mean horizontal component of peak and spectral ground motion parameters, PEER Report, College of Engineering University of California, Berkeley, USA
- Bradley BA, Baker JW (2014) Ground motion directionality in the 2010–2011 Canterbury earthquakes, Earthquake Engineering and structural Dynamics
- Bulajic B, Manic M (2005) Motion records as a seismological input for seismic safety evaluation engineering structures. Conference Paper on Strong Ground Motion, Engineering Seismology, Earthquake Hazards and Risk Assessment.
- Chiou BSI, Young RR (2006) Empirical ground motion model for the average horizontal component of peak acceleration

- and pseudo-spectral acceleration for spectral period 0.01 to 10 s, Interim Report for USGS Review
- Cornell CA (1978) Engineering seismic risk analysis. *Bull Seismol Soc Am* 58(5):1583–1606
- Cotton F, Scherbaum F, Bommer JJ, Bungum H (2006) Criteria for selecting and adjusting ground-motion models for specific target regions: application to central Europe and rock sites. *J Seismolog* 10(2):137–156
- Daryono (2011), Indeks kerentanan seismik berdasarkan mikrotremor pada setiap satuan bentuk lahan di zona Graben Bantul, Daerah Istimewa Yogyakarta, Ph.D Thesis, Gadjah Mada University (in Bahasa)
- Delavaud E, Cotton F, Akkar S, Scherbaum F, Danciu L, Beauval C, Drouet S, Douglas J, Basili R, Sandikkaya MA, Segou M, Faccioli E, Theodoulidis N (2012) Toward a ground-motion logic tree for probabilistic seismic hazard assessment in Europe. *J Seismol* 16(3):451–473
- Douglas J, Faccioli E, Cotton F, Cauzzi C (2009) Selection of ground-motion prediction equations for GEM1. *Earthquake*, No. September, pp 1–3
- Febriani F (2015) Sunsurface structure of Cimandiri fault zone, West Java Indonesia, Ph.D. Thesis, Graduate School of Science, Chiba University, p 163
- Fema p-1050-1 (2015) NEHRP recommended seismic provisions for new building and other structures, p 514
- Foulser-Piggott R (2014) Quantifying the epistemic uncertainty in ground motion models and prediction. *Soil Dyn Earthq Eng* 65:256–268
- Gerami M, Abdollahzadeh D (2012) Estimation of forward directivity effects on design spectra in near field or fault. *J Appl Sci Res* 2(9):8670–8687
- Grimaz S, Malisan P (2014) Near field domain effects and their consideration in the international and Italian seismic code. *Bolletino Di Geofisica Teorica Ed Applicata* 55(4):717–738
- Hara A, Ohta T, Niwa M, Tanaka S, Banno T (1974) Shear modulus and shear strength of cohesive soils. *Soils Foundat* 14:1–12
- Hasancebi N, Ulusay R (2006) Empirical correlations between shear wave velocity and penetration resistance for ground shaking assessment. *Bulletin Eng Geol Environ* 66:203–213
- Huang YN, Whittaker AS, Luco N (2008) Maximum spectral demand in near fault region. *Earthq Spectra* 24(1):319–341
- Imai T (1977) P and S-wave velocity of the ground in Japan, *Proceeding of the 9th International Conference on Soil Mechanics and Foundation Engineering*, Tokyo, Vol 2, pp 257–260
- Irsyam M, Widiantoro S, Natawidjaya D.H, Meilano I, Rudyanto A, Hidayati S, Triyoso W, Hanifa N.R, Djarwadi D, Faisal L, Sunarjito (2017) Peta Sumber dan Bahaya Gempa Indonesia 2017, Pusat Studi Gempa Nasional Pusat Litbang Perumahan dan Pemukiman, p 376
- Ji K, Ren Y, Wen R (2017) Site Classification for National Strong Motion Observation Network System (NSMONS) Stations in China using an empirical H/V spectral ratio method. *J Asian Earth Sci* 147:79–94
- Kalkan E, Gulkan P (2004) Empirical attenuation equation for vertical ground motion in Turkey. *Earthq Spectra* 20(3):853–882
- Kamai R, Abrahamson N (2015) Are near-fault fling effects captured in the new NGA West-2 ground motion model? *Earthq Spectra* 31(3):1629–1645
- Kempton JJ, Stewart JP (2006) Prediction equation for significant duration of earthquake ground motions considering site and near source effects. *Earthq Spectra* 22(4):985–1013
- Kukusho T, Sato K (2008) Site amplification formula for seismic zonation based on downhole array records during strong earthquakes. In: *The 14th world conference on earthquake engineering*, Beijing, China
- Kumar A, Harinarayan NH, Baro O (2015) High amplification factor for low amplitude ground motion: assessment for Delhi. *Disaster Adv* 8(12):1–11
- Kyaw ZL, Pramumijoyo S, Husein S, Fathani T, Kiyono J, Putra RR (2014) Estimation of subsurface soil layers using H/V spectrum of densely measured microtremor observations (case study: Yogyakarta City, Central Java-Indonesia). *Int J Sustain Future Huma Secur* 2(1):13–20
- Makrup LL (2009) Pengembangan Peta Deagregasi Hazard untuk Indonesia Melalui Pembuatan Software dengan Pemodelan Sumber Gempa 3-Dimensi (3-D), Disertasi Doktor Institut Teknologi Bandung, p 235 (in Bahasa)
- Maniatakis ChA, Taflampas IM, Spyarakos CC (2008) Identification of near fault earthquake record characteristics. In: *The 14th world conference of earthquake Engineering*, Beijing, China
- Nguyen N, Griffin J, Cipta A, Cummins PR (2015) Indonesia's historical earthquake, geoscience, Australia, p 79
- Nurwihastuti DW, Sartohadi J, Mardiatno D, Nehren U, Restu (2014) Understanding of earthquake damage pattern through geomorphological approach: a case study of 2006 earthquake in Bantul, Yogyakarta, Indonesia. *World J Eng Technol* 2(3):61–70
- Ohta T, Hara A, Niwa M, Sakano T (1972) Elastic modulus of soil deposits estimated by N-value. In: *Proceeding of the 7th Annual Conference. The Japanese Society of Soil Mechanics and Foundation Engineering*, pp 265–268
- Park DP, Hashash YMA (2004) Estimation of nonlinear site effects for deep soil deposits of the Mississippi Embayment, National Science Foundation Report, Mid America Earthquake Center, p 254
- Partono W, Irsyam M, Wardani SPR (2017) Development of site class and site coefficient maps of Semarang, Indonesia, using field shear wave velocity data. *MATEC Web Conf* 101:01010
- Perdhana R, Nurchahya BE (2019) Seismic microzonation base don microseismic data and damage distribution of 2006 Yogyakarta earthquake. *E3S Web Conf* 76:1–4
- Presti DCFL, Lai CG, Puci I, ONDA (2006) Computer code for nonlinear seismic response analysis of soil deposits. *J Geotech Geoenviron Eng ASCE* 223–236
- Rezaeian S, Kiureghian AD (2010) Simulation of synthetic ground motion for specific earthquake and site characteristics. *Earthq Eng Struct Dyn* 39:1155–1180
- Sadigh K, Chang CY, Egan JA, Makdisi F, Young RR (1997) Attenuation relationships for shallow crustal earthquake based on California strong motion data, *Seismological Reserach Letter Vol 68*, Seismological Society of America
- Sengara IW, Komerdevi D (2019) Site specific response analysis (SSRA) and Pairs of Ground Motions Time History

- Generations of a Site in Jakarta. In: The 4th international conference on earthquake engineering and disaster management, Padang Indonesia
- Shiuly A, Sahu RB, Mandal S (2014) Effects of soil and ground amplification of Kalkota City. *Int J Geotech Earthq Eng* 5(1):1–20
- Stanko D, Markusic S, Gazdek M, Sankovic C, Slukan I, Ivancic I (2019) Assessment of seismic site amplification in the City of Ivanec (NW part of Croatia) using the microtremor HVSR method and equivalent linear site response analysis. *Geoscience* 9(312):1–27
- Stewart JP, Chiou SJ, Bray JD, Somerville PG, Abrahamson N (2001) Ground motion evaluation procedures for performance based design. *Pacific Earthquake Engineering Research Center, PEER 2001*, p 229
- Stewart JP et al (2015) Selection of ground motion prediction equations for the global earthquake model. *Earthq Spectra* 31(1):19–45
- Strasser F, Bommer JJ, Abrahamson N (2008) Estimating ground-motion variability: issues, insights & challenges. In: The 14th world conference on earthquake engineering
- Sunardi B (2016) Percepatan Tanah sintetis kota Yogyakarta berdasarkan Deagregasi Bahaya Gempa. *J Lingkungan Dan Bencana Geologi* 6(2):211–218 (**in Bahasa**)
- Widodo P (2018) The estimated of PGA map of the Mw6.4 Yogyakarta, Indonesia earthquake constructed from modified Mercalli Intensity Imm. *Bull N Z Soc Earthq Eng* 51(2):92–104
- Widodo P (2020) Middle value ground acceleration map and site effect in the Merapi sedimentary Basin Under the 2006 Yogyakarta, Indonesia Earthquake. *Nat Hazards* 102:419–443
- Widodo P, Makrup L, Teguh M, Suryo B, Hartantyo E (2019) Site coefficient of short Fa and long period Fv maps constructed from the probabilistic seismic hazard analysis in Yogyakarta Special Province. *MATEC Web Conf* 280(01001):1–17
- Yahyai M, Rezayibana B, Muhammadrezapour E (2011) Effect of near fault earthquakes with forward directivity in telecommunication towers. *Earthq Eng Vib* 10:211–218

Publisher's Note Springer Nature remains neutral with regard to jurisdictional claims in published maps and institutional affiliations.

Springer Nature or its licensor holds exclusive rights to this article under a publishing agreement with the author(s) or other rightsholder(s); author self-archiving of the accepted manuscript version of this article is solely governed by the terms of such publishing agreement and applicable law.